JOURNAL OF MATERIALS SCIENCE **34** (1999) 3315–3326

Correlation of stepwise fatigue and creep slow crack growth in high density polyethylene

M. PARSONS, E. V. STEPANOV, A. HILTNER*, E. BAER
Department of Macromolecular Science and the Center for Applied Polymer Research, Case Western Reserve University, Cleveland, OH 44106-7202, USA

The kinetics and mechanism of slow crack growth in fatigue and creep of high density polyethylene were studied. The relationship between fatigue and creep was examined by varying the R-ratio (the minimum/maximum loads in the fatigue loading cycle) in the tensile mode such that loading ranged from mainly dynamic ($R = 0.1$) to static ($R = 1.0$, creep test). The stepwise crack propagation mechanism characteristic of long-term failures in polyethylene was observed for all loading conditions studied. Fatigue fracture kinetics allowed for extrapolation to the case of creep failure, which suggested that short-term fatigue testing can be used to predict long-term creep fracture properties. The size of the craze damage zone ahead of the arrested crack tip was controlled only by the mean stress, however the lifetime of the zone was determined by both the maximum stress and the mean stress. Crack growth rate was related to the maximum stress and the mean stress by a power law relationship, which described crack growth over the entire range of loading conditions studied.

1. Introduction

Long-term failures of structural materials often occur by slow crack growth under loads that are well below the yield stress of the material. Testing materials under exact field conditions is impractical because of the very long failure times, so prediction of long-term failure from short-term tests is desirable. However, reliable prediction requires the mechanism of long-term failure to be maintained while the crack growth rate is substantially accelerated.

Prediction of slow crack growth in polyethylene pipes used for natural gas distribution is an example where short-term testing is vitally needed. In the field, failure occurs under mainly static loads. Elevating the test temperature is one method of accelerating failure, and a high temperature creep test (PENT test) was designed specifically for predicting long-term failure of gas-pipe resins [1]. Another method of accelerating failure is fatigue testing. A fatigue testing protocol was developed that reproduced the stepwise crack growth mechanism observed in field failures, and enabled ranking of polyethylene pipe resins in the same order as the PENT test but in up to three orders of magnitude less time [2–6]. Fatigue testing was carried out at ambient temperature which avoided possible annealing effects inherent to polymers at elevated temperature. However, only a qualitative assessment of long-term creep failure could be made from dynamic fatigue testing.

The relationship between fatigue and creep can be quantitatively examined by systematically decreasing the dynamic component of fatigue loading. This can be accomplished by varying the R-ratio, defined as the ratio of the minimum stress to the maximum stress in the fatigue loading cycle, so that R gradually approaches unity (creep loading). The R-ratio can be varied under conditions of constant maximum load or constant mean load, Fig. 1.

The basis for using dynamic fatigue testing to predict fracture properties under mainly static loads is the demonstration of correlation of fracture kinetics and mechanism in fatigue and creep tests. If a correlation is found, then a single model relating slow crack growth rate to applied stress intensity factor can be developed that describes both fatigue and creep loading. In a creep test, stress intensity factor can be expressed as a single parameter K_I. In a fatigue test, multiple parameters such as $K_{I,max}$, $K_{I,min}$, $K_{I,mean}$, ΔK_I, and R are needed to describe the cyclic loading. Crack growth rate in the fatigue test is typically related to the applied stress by the Paris relation [2–4, 7–11]: $da/dt = A\Delta K_I^n$, where crack growth rate (da/dt) is the change in crack length (da) with time (dt); and the parameter A and the exponent n are material characteristics. The Paris relation has been applied to both continuous crack growth, where the crack advances every loading cycle, and to discontinuous crack growth, where the crack is arrested for up to many tens of thousands of cycles and then advances over a period of up to a few thousand cycles [2–4, 7, 12].

Although ΔK_I is often the primary factor governing fatigue crack growth, for polymers $K_{I,max}$, $K_{I,mean}$, ΔK_I, and R have all been shown to correlate with crack

* Author to whom all correspondence should be addressed.

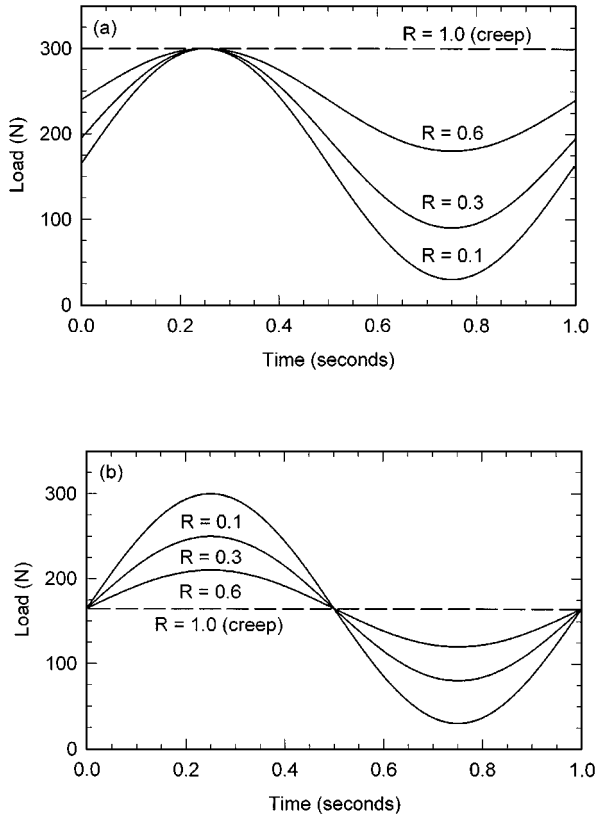

Figure 1 Fatigue loading for different R-ratios under (a) constant $K_{I,max}$ and (b) constant $K_{I,mean}$ loading.

growth rate [7–9, 12–14]. Other relations where stress intensity factor is represented by one or more of these parameters have been proposed [13, 14], but none has gained universal acceptance in describing fatigue crack growth [7]. It is realized that the Paris relation and other Paris-type relations where stress intensity factor is represented by ΔK_I are not applicable to creep testing where $\Delta K_I = 0$.

The effect of R on fatigue crack growth is of particular interest because by varying R the relative contributions of the static and dynamic loading components can be manipulated. Previous studies have shown that the effect of R on fatigue crack growth is quite complex. In a study where R was varied between 0.1 and 0.5 under conditions of constant ΔK_I, crack growth rate increased with increasing R in some polymers and decreased with increasing R in others [7, 13–19]. However, varying R under constant ΔK_I limits the experiments to a small range of R if the slow crack growth mechanism is to be maintained, because increasing R requires a large increase in $K_{I,max}$ [7].

Under constant $K_{I,max}$ loading, crack growth rate in high density polyethylene (HDPE) was observed to increase between $R = -1.0$ and 0.5, and to decrease between $R = 0.5$ and 1.0 [20]. Furthermore, applying the minimum load in compression ($R < 0$) resulted in additional damage from bending and breakage of craze fibrils [20, 21]. In this study fracture was continuous and ductile, so the results are not directly applicable to predicting stepwise brittle-type fracture of HDPE.

In another study using constant $K_{I,max}$ loading, crack growth rate in one polyethylene resin decreased exponentially with increasing R between 0.1 and 1.0, and in another resin crack growth ceased when R was raised to 0.5 [22]. In the study, R-ratio was varied during the test. Because discontinuous crack propagation in polyethylene proceeds by the sequential formation and fracture of a craze damage zone at the crack tip, changing R during the test could lead to ambiguous results if the craze zone formed under one loading condition and then fractured under another.

An experimental protocol to examine the relationship between fatigue and creep requires loading conditions that produce the same crack growth mechanism in fatigue and creep. Fatigue loading must be restricted to the tensile mode to avoid compressive damage of the craze fibrils. Additionally, a wide range of fatigue and creep loading conditions is needed so that the relative effects of the individual stress intensity factor parameters $K_{I,max}$, $K_{I,min}$, $K_{I,mean}$, ΔK_I, and R can be distinguished.

The goal of the present work was to extend the results of previous studies that showed a qualitative correlation between fatigue and creep crack growth in polyethylene [2–6]. In these studies R was held constant at 0.1, and the maximum stress was varied. In the present study a quantitative comparison between fatigue and creep of HDPE was made by varying the R-ratio under conditions of both constant $K_{I,max}$ and constant $K_{I,mean}$ loading. A HDPE resin was used because it fails by the stepwise crack propagation mechanism common in pipe resins but exhibits faster crack growth.

2. Experimental

2.1. Materials

The material used in this study was the high density polyethylene (HDPE) used previously [2]. The weight average molecular weight was 360000 g/mol, the polydispersity was 12, the density was 955 kg/m^3, and the crystallinity was 72%.

To obtain compression molded plaques about 17 mm thick, the resin was preheated at 190 °C between Mylar sheets in a press; a pressure of 20 MPa was applied for 15 minutes; the pressure was rapidly cycled 10 times between 20 and 40 MPa to remove any air bubbles which could have led to voids, and the pressure was maintained at 40 MPa for an additional 5 minutes. Plaques were cooled under pressure at a nominal rate of about 30 °C/min by circulating cold water through the platens. Water circulation was maintained for an additional 30 minutes after the platens reached room temperature to ensure that the center of the plaques had cooled completely. Plaques were machined to a thickness of 13 mm. Compact tension specimens, with dimensions in compliance with ASTM D 5045–93, were cut from the plaques. Schematics illustrating the geometry and dimensions were presented previously [5]. The length, defined as the distance between the line connecting the centers of the loading pin holes and the unnotched outer edge of the specimen, was 26 mm. The height to length ratio was 1.2, and the notch length was 12.5 mm. Specimens were notched in two steps: the initial 10 mm were made by saw, and the final 2.5 mm by razor blade. The razor blade was driven into the specimen at a controlled

rate of 1 μm/s. A fresh razor blade was used for each specimen.

2.2. Fatigue and creep testing

Mechanical fatigue units capable of applying a very stable and accurate ($\pm$0.5N) sinusoidal load were used to conduct fatigue tests. The load and crosshead displacement were recorded by computer every 1000 cycles. A manual zoom macrolens attached to a video camera was used to observe the crack tip. The camera was routed through a VCR and video monitor and, when the test was left unattended, the experiment was recorded onto video cassette. The crack tip opening displacement (CTOD), defined as the maximum craze opening at the peak of the fatigue loading cycle, was taken from the video. The CTOD could only be measured for the first craze zone. In subsequent zones the top and bottom of the craze were obscured by fractured fibrils remaining from the first craze.

The R-ratio, defined as the ratio of minimum to maximum loads in the fatigue loading cycle, was varied from 0.1 to 1.0 (creep). Tests were done under conditions of constant maximum stress and constant mean stress. Two maximum stresses, $K_{\mathrm{I,max}} = 1.30$ and 1.08 MPa(m)$^{1/2}$, were used. Under constant maximum stress, R was increased by increasing the minimum stress, Fig. 1a. Two mean stresses, 0.85 and 0.72 MPa(m)$^{1/2}$, were used. Under constant mean stress, R was increased by decreasing the maximum stress and increasing the minimum stress, Fig. 1b. In addition, fatigue experiments were performed under constant $R = 0.1$ and varying $K_{\mathrm{I,max}}$ from 0.91 to 1.30 MPa(m)$^{1/2}$. The entire matrix of fatigue and creep experiments is shown in Tables I–III. The test frequency was 1 Hz.

TABLE I Crack growth kinetics under constant $K_{\mathrm{I,max}}$ loading

No. of trials	R	$K_{\mathrm{I,max}}$ MPa(m)$^{1/2}$	$K_{\mathrm{I,mean}}$ MPa(m)$^{1/2}$	Time to 1st crack jump, t_1 seconds $\times 10^3$	Time to 2nd crack jump, t_{2+1} seconds $\times 10^3$	Time to fracture, t_{f} seconds $\times 10^3$
3	0.10	1.30	0.72	32 ± 2	58 ± 2	153 ± 19
2	0.20	1.30	0.78	36 ± 6	68 ± 10	162 ± 27
2	0.30	1.30	0.85	54 ± 16	103 ± 18	228 ± 32
2	0.40	1.30	0.91	70 ± 7	138 ± 11	264 ± 35
2	0.50	1.30	0.98	84 ± 2	150 ± 7	322 ± 47
3	0.60	1.30	1.04	76 ± 9	141 ± 2	313 ± 43
2	0.70	1.30	1.10	96 ± 8	168 ± 11	361 ± 50
2	0.80	1.30	1.17	94 ± 2	176 ± 2	383 ± 34
2	1.00	1.30	1.30	135 ± 21	220 ± 14	403 ± 52
2	0.10	1.08	0.60	48 ± 4	85 ± 7	386 ± 34
2	0.32	1.08	0.72	98 ± 15	169 ± 15	590 ± 32
2	0.50	1.08	0.82	123 ± 16	213 ± 38	660 ± 55
2	1.00	1.08	1.08	168 ± 11	278 ± 4	864 ± 61

TABLE II Crack growth kinetics under constant $K_{\mathrm{I,mean}}$ loading

No. of trials	R	$K_{\mathrm{I,max}}$ MPa(m)$^{1/2}$	$K_{\mathrm{I,mean}}$ MPa(m)$^{1/2}$	Time to 1st crack jump, t_1 seconds $\times 10^3$	Time to 2nd crack jump, t_{2+1} seconds $\times 10^3$	Time to fracture, t_{f} seconds $\times 10^3$
2	0.20	1.43	0.85	33 ± 3	60 ± 7	135 ± 2
2	0.30	1.30	0.85	54 ± 16	103 ± 18	228 ± 32
2	0.50	1.13	0.85	121 ± 8	196 ± 8	570 ± 3
2	1.00	0.85	0.85	421 ± 30	701 ± 2	$2,065 \pm 290$
3	0.10	1.30	0.72	32 ± 2	58 ± 2	153 ± 19
2	0.22	1.17	0.72	64 ± 4	114 ± 8	297 ± 25
2	0.32	1.08	0.72	98 ± 15	169 ± 15	590 ± 32
2	0.43	1.00	0.72	165 ± 21	255 ± 40	(a)
2	0.57	0.91	0.72	295 ± 49	475 ± 55	(a)
1	0.72	0.83	0.72	400	720	(a)
1	1.00	0.72	0.72	605	1,040	3,400

(a) Tests were stopped before fracture

TABLE III Crack growth kinetics under constant $R = 0.1$ loading

No. of trials	R	$K_{\mathrm{I,max}}$ MPa(m)$^{1/2}$	$K_{\mathrm{I,mean}}$ MPa(m)$^{1/2}$	Time to 1st crack jump, t_1 seconds $\times 10^3$	Time to 2nd crack jump, t_{2+1} seconds $\times 10^3$	Time to fracture, t_{f} seconds $\times 10^3$
2	0.10	1.30	0.72	32 ± 2	58 ± 2	153 ± 19
2	0.10	1.08	0.60	48 ± 4	85 ± 7	386 ± 34
1	0.10	1.00	0.55	55	95	551
1	0.10	0.91	0.50	85	160	735

Fracture surfaces were examined under the light microscope to measure step jump length. Features were best resolved in bright field using normal incidence illumination. Specimens were subsequently coated with 9 nm of gold and examined in a JEOL JSM 840A scanning electron microscope. The accelerator voltage was set at 5 kV and the probe current at 6×10^{-11} A to minimize radiation damage to the specimens.

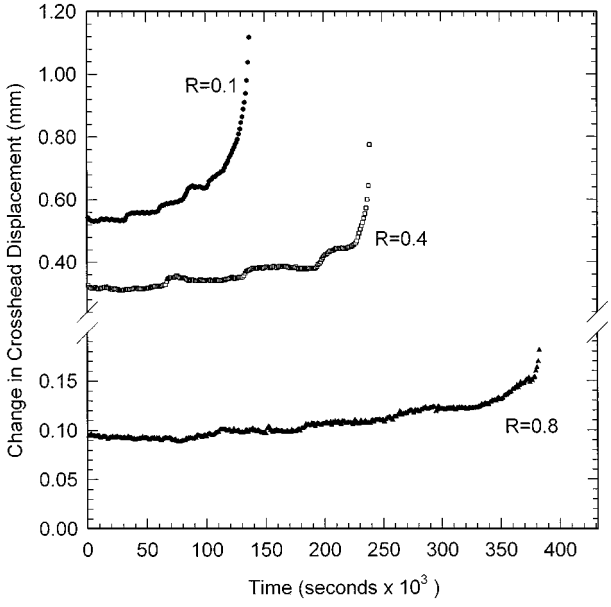

Figure 2 Typical crosshead displacement curves for fatigue tests under different R-ratios with $K_{I,max} = 1.30\,MPa(m)^{1/2}$.

To test whether step jump length correlated with craze zone length, two specimens, one with $R = 0.1$ and the other with $R = 1.0$ (creep test), were loaded under $K_{I,max} = 1.30\ MPa(m)^{1/2}$ to the point where voids were first observed in the membrane. At this point the damage zone had reached maximum length but the crack had yet to jump through the zone. The specimens were sectioned to reveal the damage zone. For both $R = 0.1$ and $R = 1.0$ the damage zone length corresponded to the step jump length.

3. Results and discussion

3.1. Slow crack growth under constant $K_{I,max}$ loading

Typical plots of change in crosshead displacement, defined as the difference in maximum and minimum positions in the fatigue cycle, are shown in Fig. 2 for $K_{I,max} = 1.30\,MPa(m)^{1/2}$ and $R = 0.1$, 0.4, and 0.8. The corresponding fatigue fracture surfaces for $R = 0.1$, 0.4, 0.8 are compared with the creep fracture surface ($R = 1$) in Fig. 3. The stepwise character

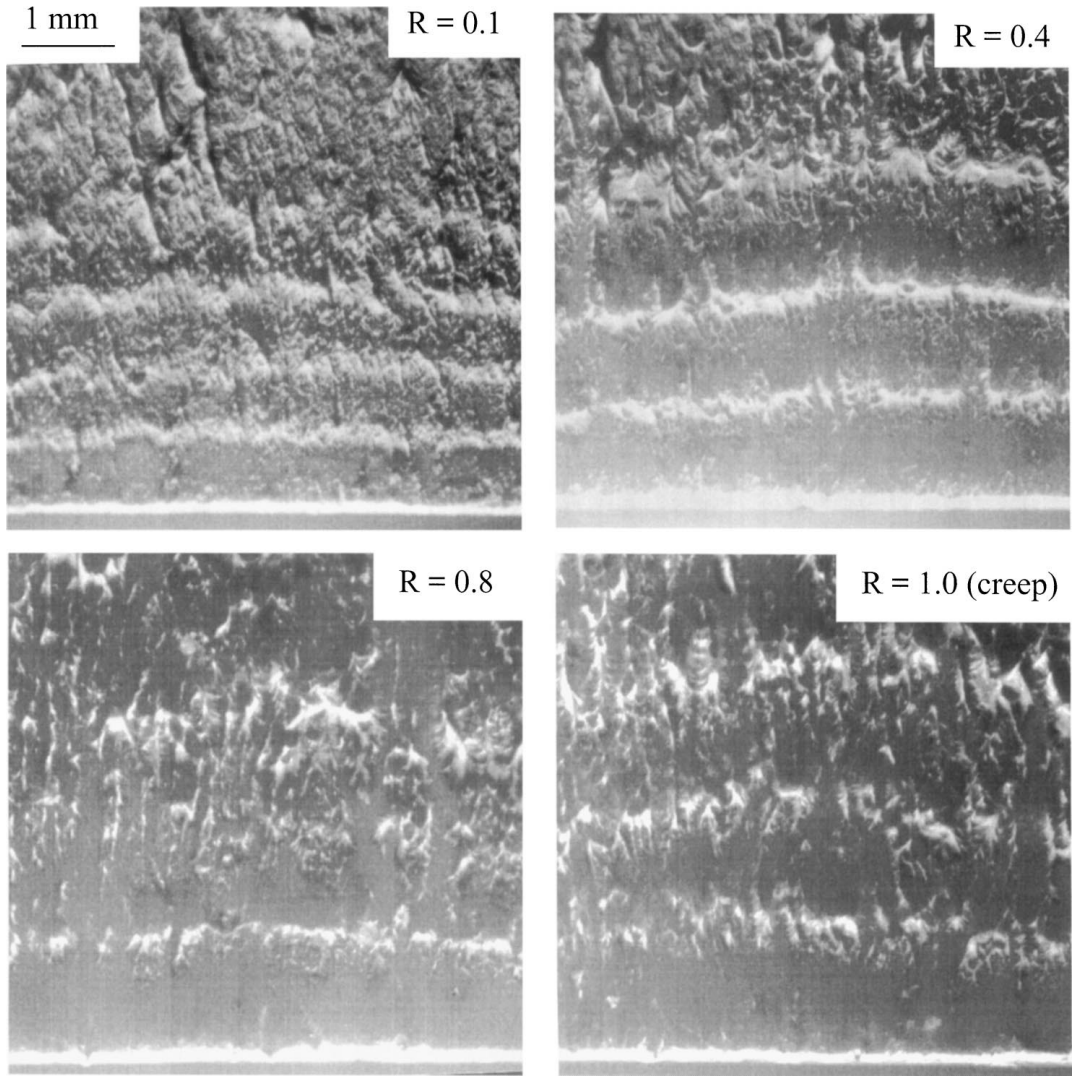

Figure 3 Fracture surfaces of specimens tested under $K_{I,max} = 1.30\,MPa(m)^{1/2}$ and $R = 0.1$, 0.4, 0.8 and 1.0.

of crack growth resulting from the sequential formation and fracture of craze damage zones was well resolved on the plots and the fracture surfaces. The plateaus in Fig. 2 corresponded to arrest periods, during which a damage zone formed in order to relieve the stress concentration at the crack tip. The damage zone consisted of a main craze with a continuous membrane at the crack tip. The duration of the arrest period, which encompassed tens of thousands of seconds, corresponded to the lifetime of the damage zone. Near the end of the arrest period, the main part of the craze broke down, leaving the continuous membrane at the crack tip. The membrane then ruptured within a few thousand cycles by a process of void formation and coalescence. A sharp increase in crosshead displacement followed membrane rupture, Fig. 2. Remnants of the broken membrane fibrils made up the prominent striations visible on the fracture surfaces, Fig. 3. The stepwise crack growth mechanism, which was the same as reported in previous studies [2–6], was observed over the entire range of R-ratios and stress intensity factors examined.

The number of striations corresponded to the number of step jumps observed on the crosshead displacement curves in Fig. 2. The number decreased from 5 for $R = 0.1$ to 4 for $R = 0.4$ and $R = 0.8$, and to 3 for the creep test ($R = 1.0$). The 5 steps for $R = 0.1$ is consistent with previous observations made under the same loading conditions for this material [5]. With increasing R-ratio the step jump length increased. The total number of steps decreased, however, so that the total length of the stepwise crack growth region remained nearly constant. On each fracture surface, the distance between successive jumps increased because the stress intensity factor increased as the crack became longer [5]. When the stress intensity factor reached the limit of brittle fracture, rapid ductile failure ensued.

Higher magnification SEM micrographs of the first craze zone on the fracture surfaces in Fig. 3 are shown in Fig. 4. For all R-ratios, the surface consisted of dense, uniaxially drawn fibrils less than 1 μm thick. This suggested that the craze morphology was not affected by changes in the loading conditions. The same features were observed on the fracture surfaces of specimens loaded under constant $K_{\mathrm{I,mean}}$. For all the loading conditions used in this study, the crack propagated in a stepwise manner through a fibrous craze.

Optical micrographs of fracture surfaces from tests under a lower $K_{\mathrm{I,max}}$ of 1.08 MPa(m)$^{1/2}$ are shown in Fig. 5 for $R = 0.1, 0.32, 0.5$, and 1.0. As was the case for $K_{\mathrm{I,max}} = 1.30$ MPa(m)$^{1/2}$ the length of the step jumps increased with increasing R-ratio. The total length of the stepwise crack propagation region was about the same as in the $K_{\mathrm{I,max}} = 1.30$ MPa(m)$^{1/2}$ tests, but there were more, shorter steps. The number of step jumps was about 11, 8, 6, and 4 for $R = 0.1$, 0.32, 0.5, and 1.0, respectively.

The durations to the first step jump, second step jump, and to fracture which are designated t_1, t_{2+1}, and t_{f} were used to characterize stepwise crack propagation. Fig. 6a and b are plots of t_1, t_{2+1}, and t_{f}, vs. R for $K_{\mathrm{I,max}} =$ 1.30 and 1.08 MPa(m)$^{1/2}$. The data are also shown in Table I. The durations were longer for the lower maximum stress, $K_{\mathrm{I,max}} = 1.08$ MPa(m)$^{1/2}$, than the higher one, $K_{\mathrm{I,max}} = 1.30$ MPa(m)$^{1/2}$. For both $K_{\mathrm{I,max}}$ values, t_1, t_{2+1}, and t_{f} increased almost linearly with

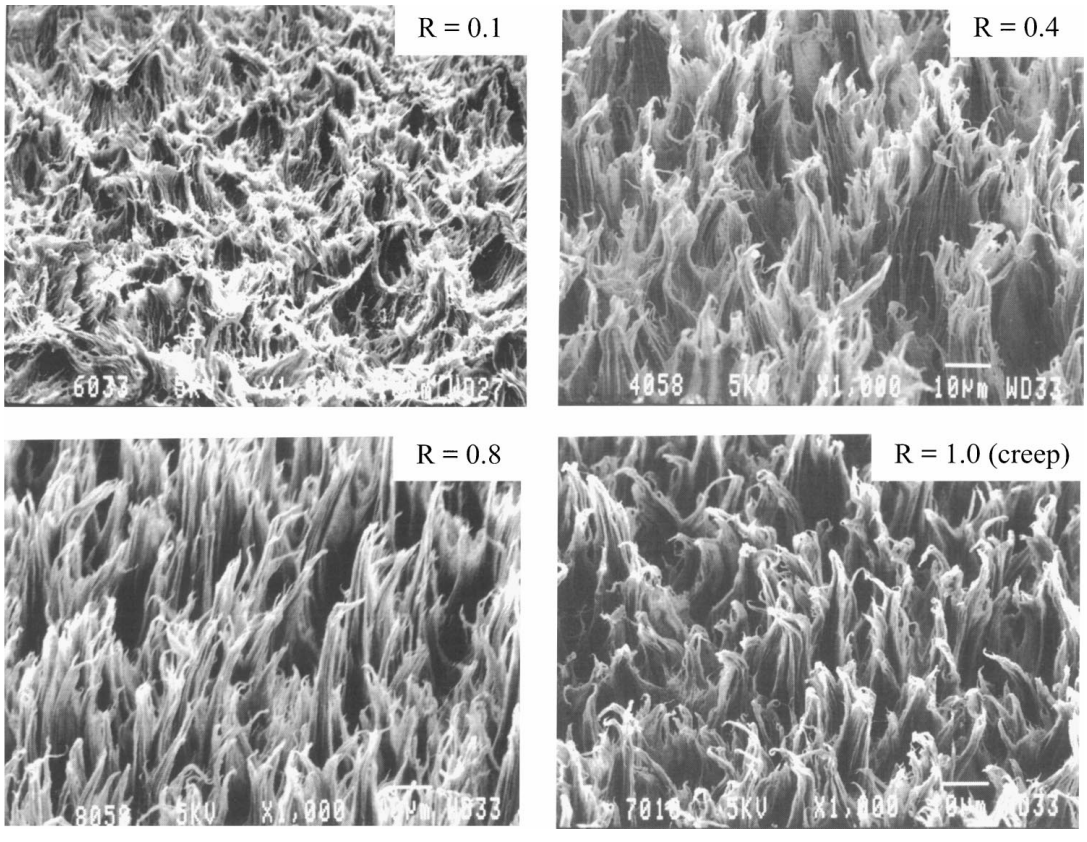

Figure 4 SEM micrographs of the first craze zone of the four fracture surfaces shown in Fig. 3.

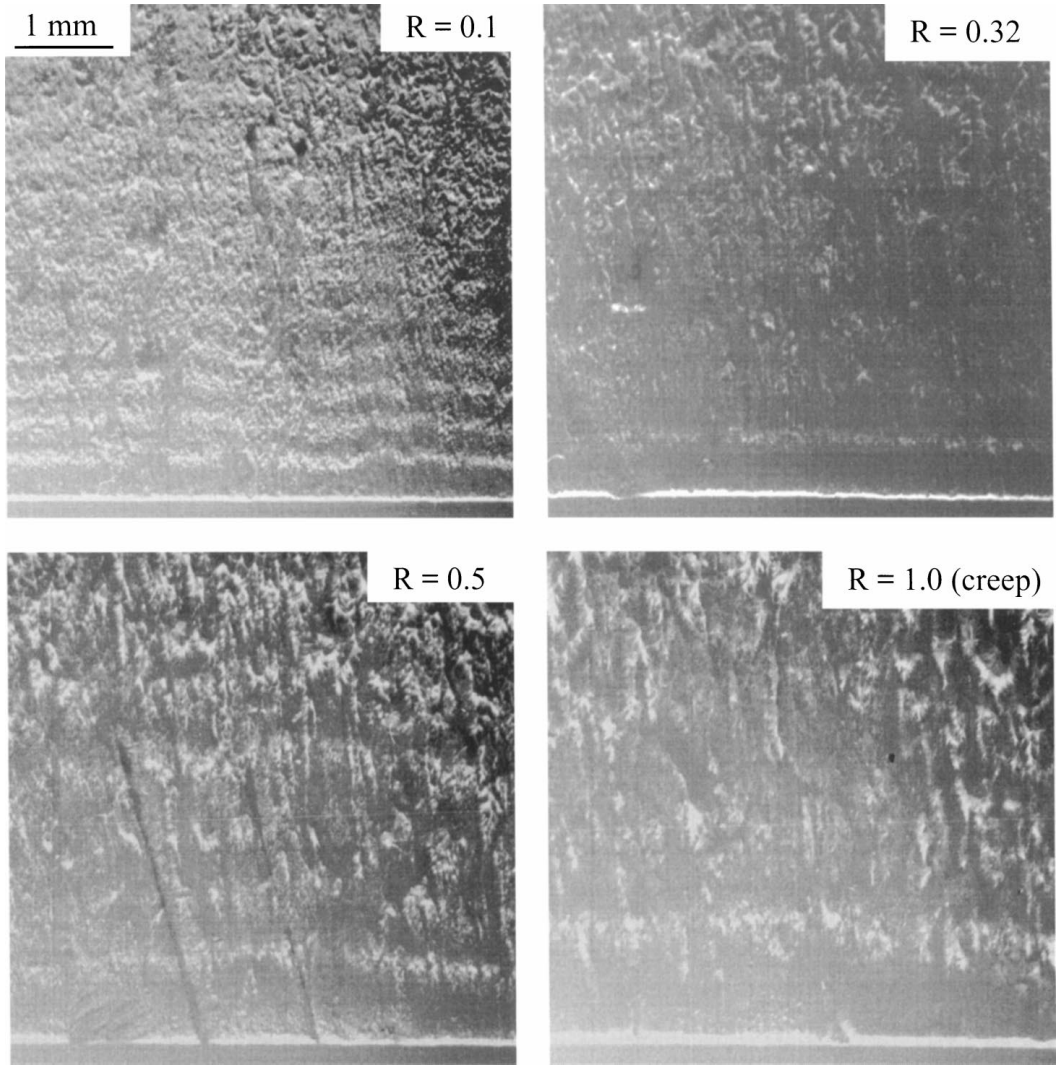

Figure 5 Fracture surfaces of specimens tested under $K_{I,max} = 1.08\,MPa(m)^{1/2}$ and $R = 0.1$, 0.32, 0.5 and 1.0.

increasing R-ratio. The conservation in stepwise crack propagation mechanism and smooth extrapolation from fatigue to creep crack growth kinetics indicated that short-term fatigue testing can predict long-term fracture in HDPE.

3.2. Slow crack growth under constant $K_{I,mean}$

Crack propagation was also examined under conditions of constant $K_{I,mean}$ and comparison was made to the constant $K_{I,max}$ tests. Optical micrographs of the fracture surfaces of specimens tested with different R-ratios under $K_{I,mean} = 0.85$ and $0.72\,MPa(m)^{1/2}$ are shown in Figs 7 and 8. As was observed in the constant $K_{I,max}$ loading, striations indicative of stepwise crack growth were apparent on the fracture surfaces. In contrast to the constant $K_{I,max}$ loading, the step jump length did not change with increasing R-ratio. For each $K_{I,mean}$ the number of step jumps was about 5. The length of the step jumps was larger for the $K_{I,mean} = 0.85\,MPa(m)^{1/2}$ than for $K_{I,mean} = 0.72\,MPa(m)^{1/2}$.

The durations to the first step jump, second step jump, and to failure are plotted vs. R-ratio in Fig. 9a and b, and shown in Table II. With increasing R-ratio, t_1, t_{2+1}, and t_f increased more sharply under constant $K_{I,mean}$ loading than under constant $K_{I,max}$ loading and, consequently, the time axis in Fig. 9 is logarithmic. For a given R-ratio, t_1, t_{2+1}, and t_f were longer for $K_{I,mean} = 0.72\,MPa(m)^{1/2}$ than for $K_{I,mean} = 0.85\,MPa(m)^{1/2}$.

3.3. Crack growth kinetics

Crack growth rate has been proposed as the best parameter to represent crack growth kinetics [2–4] because it relates directly to the size and lifetime of the damage zone. Furthermore, crack growth rate is often used to compare fatigue crack growth, both continuous and discontinuous, in polymers. Crack initiation time and total failure time have also been used to represent crack growth [21, 23–25], however crack initiation time may depend on the notching procedure [26], and failure time encompasses all the processes of crack initiation, stepwise crack growth, and final ductile fracture.

Because crack growth was discontinuous, an average crack growth rate (da/dt) was calculated as the step jump length (da) divided by the lifetime of the damage zone (dt). The effects of stress intensity factor on damage zone size and damage zone lifetime were considered separately, and then a relation governing crack growth over the entire R range was developed. The wide range of fatigue and creep loading conditions

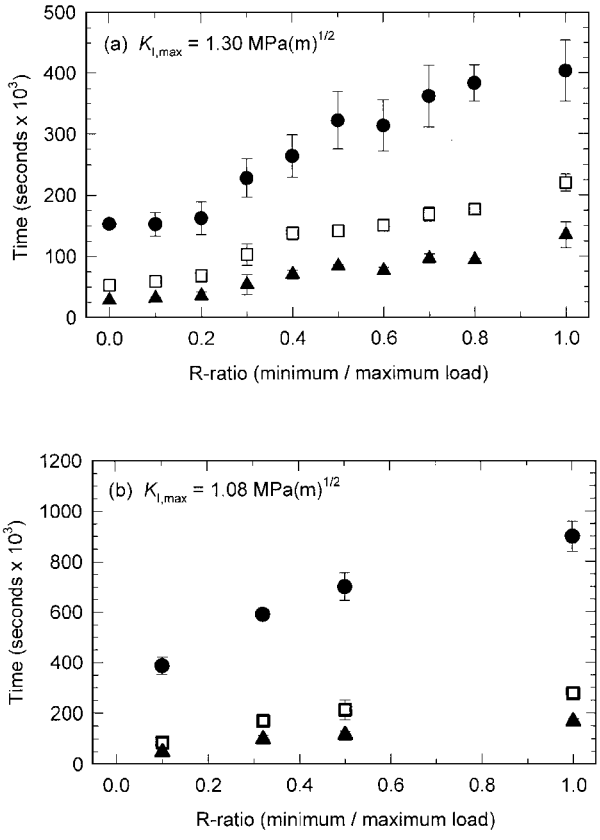

Figure 6 Effect of R-ratio on time to the first step jump t_1 (▲), second step jump t_{2+1} (□), and fracture t_f (●) for specimens loaded under a constant maximum stress of (a) $K_{I,max} = 1.30\,\text{MPa(m)}^{1/2}$ and (b) $K_{I,max} = 1.08\,\text{MPa(m)}^{1/2}$.

allowed the relative effects of the stress intensity factor parameters $K_{I,max}$, $K_{I,mean}$, ΔK_I, and R on stepwise crack growth to be distinguished.

3.4. Damage zone lifetime

The lifetime of the first damage zone may be affected by the initial notching [26], so the lifetime of the second damage zone, designated t_2 ($t_2 = t_{2+1} - t_1$) and measured as the duration between the first and second step jumps, was chosen to represent dt. A plot of $\log t_2$ vs. $\log K_{I,max}$ is shown in Fig. 10 for all data under constant $K_{I,max}$ and constant $K_{I,mean}$ loading. The dashed line represents the linear relation for creep, where $K_{I,mean} = K_{I,max}$. All the data followed the general trend of decreasing t_2 with increasing $K_{I,max}$. Under constant $K_{I,max}$, t_2 decreased with decreasing $K_{I,mean}$ and the data fell below the value of the corresponding creep test. Thus both $K_{I,mean}$ and $K_{I,max}$ affected damage zone lifetime (dt).

To obtain the relative effects of $K_{I,max}$ and $K_{I,mean}$ on damage zone lifetime $\log t_2$ was plotted against $\log K_{I,max}$ in Fig. 11a for tests under constant $K_{I,mean} = 0.85$ and $0.72\,\text{MPa(m)}^{1/2}$. The slope of the fit lines was about -4.5, which indicated that $dt \propto K_{I,max}^{-4.5}$. Fig. 11b shows the effect of $K_{I,mean}$ on damage zone lifetime by plotting $\log t_2$ against $\log K_{I,mean}$ for tests under constant $K_{I,max} = 1.30$ and $1.08\,\text{MPa(m)}^{1/2}$. From the slopes of lines fitting these data, damage zone lifetime was found to be proportional to $K_{I,mean}^2$.

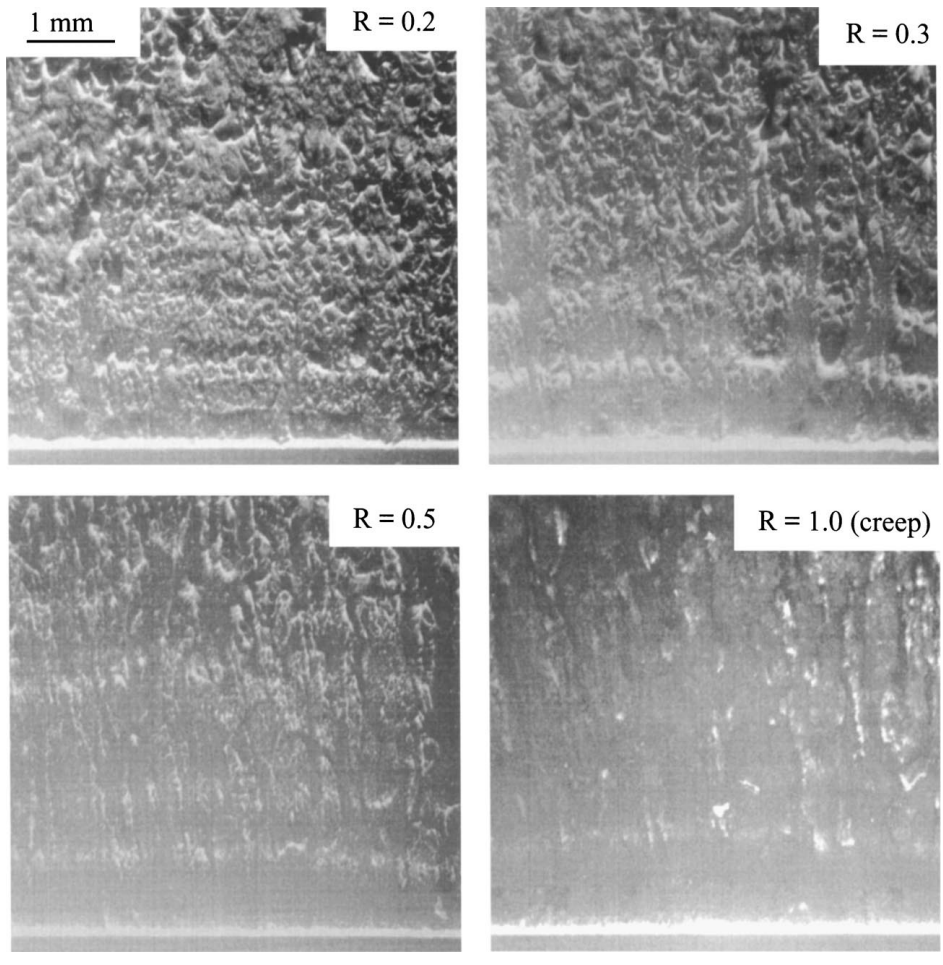

Figure 7 Fracture surfaces of specimens tested under $K_{I,mean} = 0.85\,\text{MPa(m)}^{1/2}$ and $R = 0.2$, 0.3, 0.5 and 1.0.

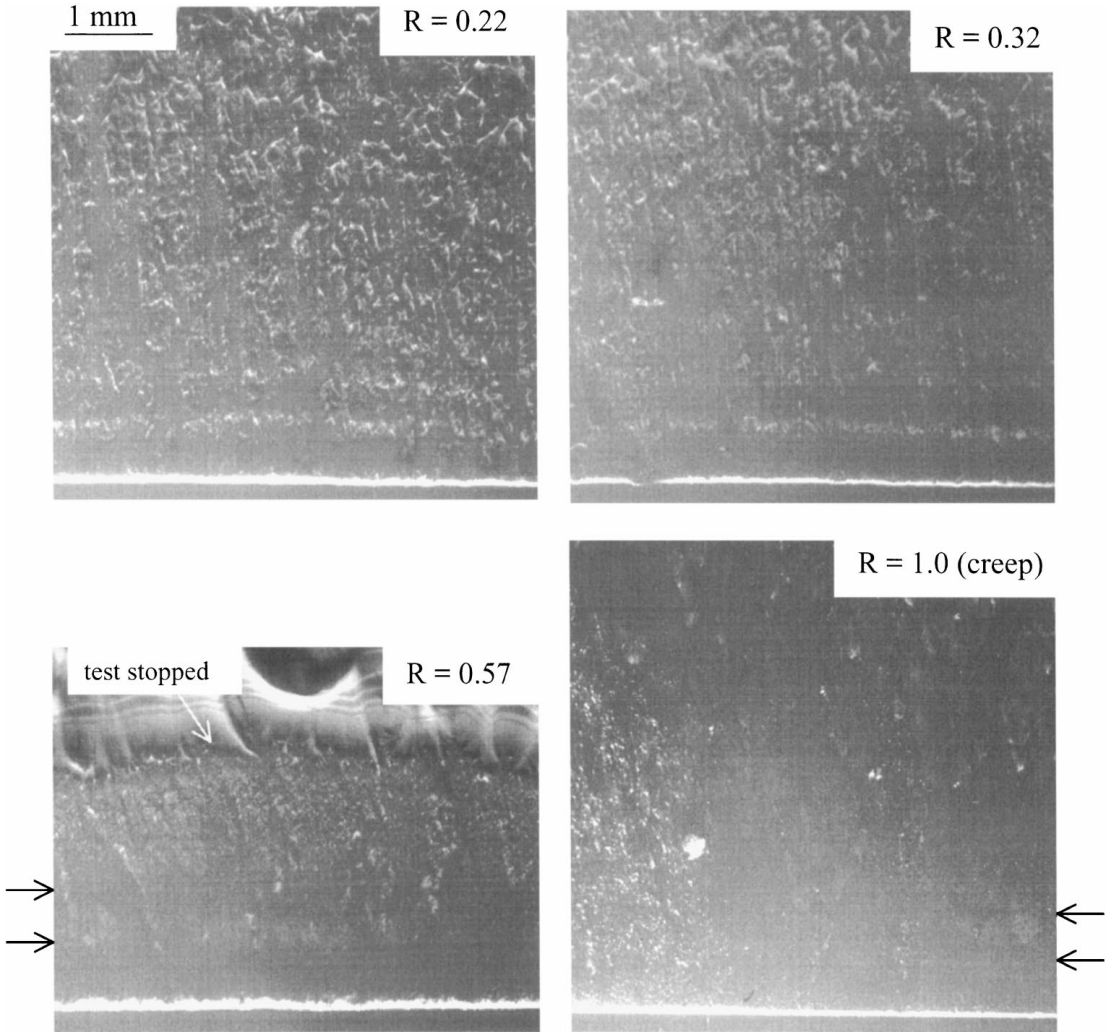

Figure 8 Fracture surfaces of specimens tested under $K_{I,mean} = 0.72\,MPa(m)^{1/2}$ and $R = 0.22$, 0.32, 0.57, and 1.0. Arrows mark the first two step jump positions on specimens where jumps were not easily distinguished on the micrographs.

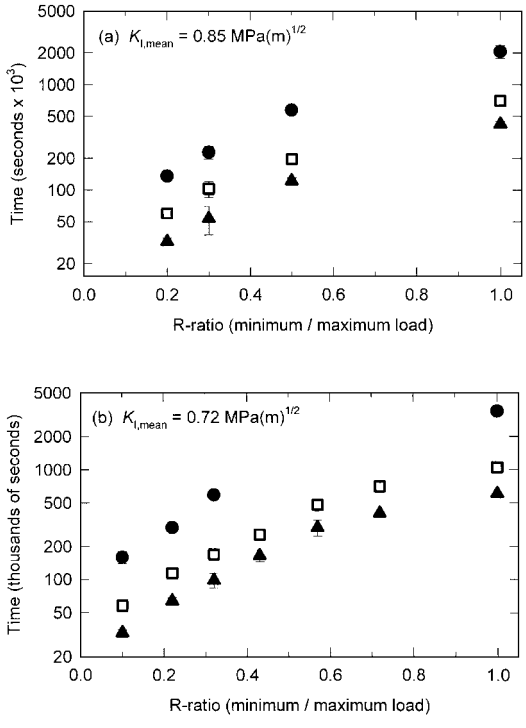

Figure 9 Effect of R-ratio on time to the first step jump t_1 (▲), second step jump t_{2+1} (□), and fracture t_f (●) for specimens loaded under a constant mean stress of (a) $K_{I,mean} = 0.85\,MPa(m)^{1/2}$ and (b) $K_{I,mean} = 0.72\,MPa(m)^{1/2}$.

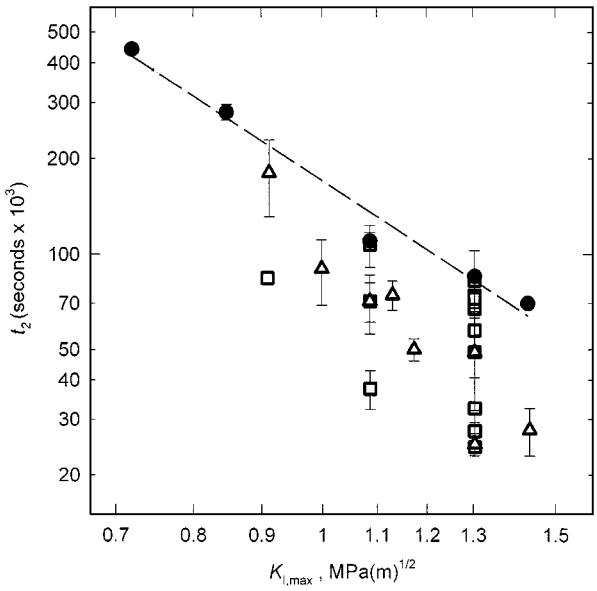

Figure 10 Effect of $K_{I,max}$ on craze zone lifetime t_2 for specimens loaded under creep (●), constant $K_{I,max}$ (□), and constant $K_{I,mean}$ (△).

3.5. Crack jump length

From the fracture surfaces of specimens tested under constant $K_{I,max}$ and constant $K_{I,mean}$ shown in Figs 3, 5, 7 and 8, it was apparent that the mean stress primarily

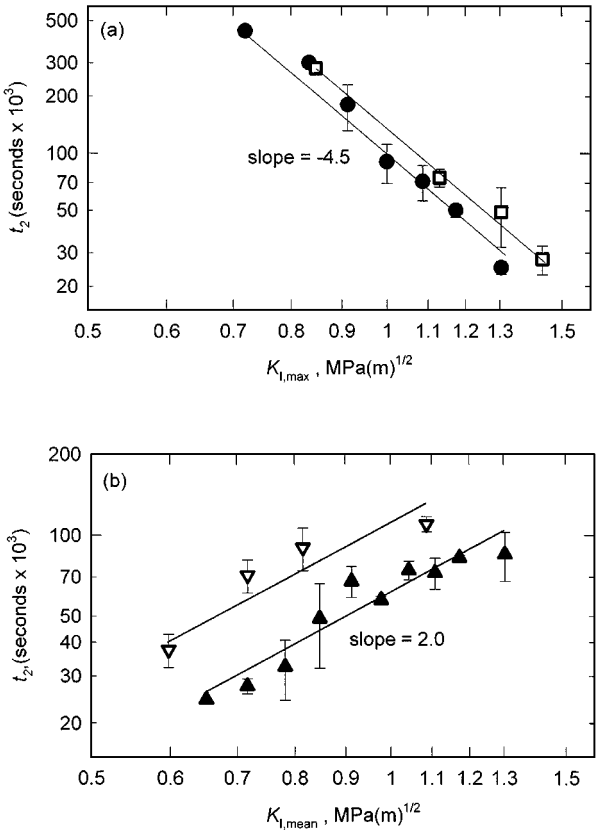

Figure 11 Effect of (a) $K_{I,max}$ on craze zone lifetime t_2 for tests under constant $K_{I,mean}$ of 0.72 MPa(m)$^{1/2}$ (●) and 0.85 MPa(m)$^{1/2}$ (□), and (b) $K_{I,mean}$ on craze zone lifetime t_2 for tests under constant $K_{I,max}$ of 1.30 MPa(m)$^{1/2}$ (▲) and $K_{I,max} = 1.08$ MPa(m)$^{1/2}$ (▽).

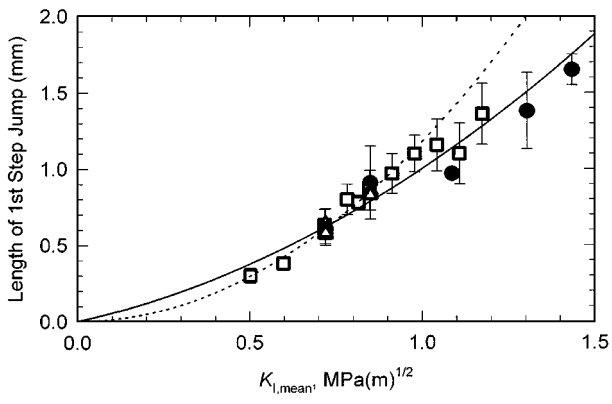

Figure 12 Effect of $K_{I,mean}$ on length of the first step jump for specimens loaded under creep (●), constant $K_{I,max}$ (□), and constant $K_{I,mean}$ (△).

controlled crack jump length. Jump length is plotted against $K_{I,mean}$ in Fig. 12. For tests under constant $K_{I,mean}$, step jump length did not change with $K_{I,max}$. Conversely, when $K_{I,max}$ was constant and $K_{I,mean}$ was varied, the step jump length increased with increasing $K_{I,mean}$.

The dependence of damage zone size on $K_{I,mean}$ rather than $K_{I,max}$ may have been a result of the time scale of craze growth. In these experiments the time required for the craze to approach the length of the step jump was on the order of 10000 to 100000 seconds. A single fatigue loading cycle, however, was completed in 1 second, which was negligible compared to the duration of craze growth. Therefore, the stress that controlled the craze length was the average during the fatigue cycle, i.e. the mean stress.

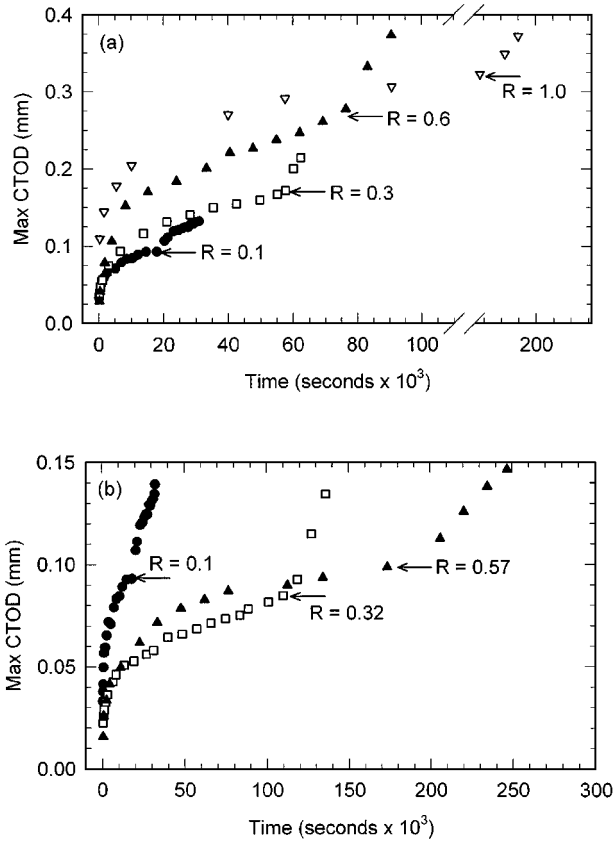

Figure 13 Effect of R-ratio on CTOD during formation and fracture of the first craze zone for loading under (a) constant $K_{I,max}$ and (b) constant $K_{I,mean}$. The arrows indicate initiation of craze fracture.

Step jump length corresponded to craze zone length. Another measure of craze size was crack tip opening displacement (CTOD), which was easily obtained by video. For specimens tested under constant $K_{I,max}$ and constant $K_{I,mean}$, the growth in CTOD of the first craze zone is shown in Fig. 13a and b. Initially CTOD increased steeply. The growth in CTOD then gradually leveled off until voids appeared in the membrane at the craze base. A rapid increase in CTOD or craze length followed by a leveling off until the crack moves is typical of fatigue of polyethylene [25] and other polymers where crack propagation is discontinuous [27]. The magnitude of the CTOD when voids were first observed increased with increasing R-ratio for constant $K_{I,max}$ loading but remained constant for constant $K_{I,mean}$ loading. The CTOD observations confirmed the notion that craze zone size was controlled by $K_{I,mean}$.

The Dugdale model [28] of the plastic zone is widely applied to relate craze zone size and shape to applied stress. The craze length (l) is given by:

$$l = \frac{\pi}{8} \cdot \frac{K_I^2}{\sigma_y^2} \tag{1}$$

where K_I is the stress intensity factor and σ_y is the yield stress. Because craze size was controlled by $K_{I,mean}$, this parameter was used to represent stress intensity factor in Equation (1). A proportionality between craze length and CTOD in Equation (1) is expected [29]. A

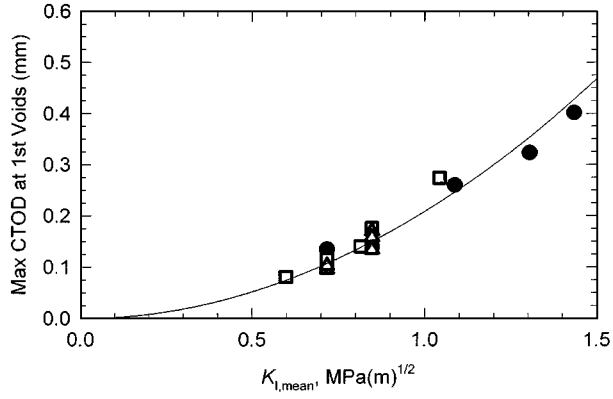

Figure 14 Effect of $K_{I,mean}$ on the CTOD at initiation of fracture of the first craze zone for specimens loaded under creep (●), constant $K_{I,max}$ (□), and constant $K_{I,mean}$ (△).

$K^2_{I,mean}$ dependence of the maximum CTOD (the CTOD just before membrane rupture) fit the data in Fig. 14 over the entire range of $K_{I,mean}$ values used. However, in contrast to CTOD, the step jump length was best fit by $da \propto K^{1.5}_{I,mean}$, which is shown as the solid line in Fig. 12.

A possible reason for the deviation in craze zone length from the predicted $K^2_{I,mean}$ dependence is that the Dugdale model assumes that the elastic stress surrounding the zone can be described by the stress intensity factor only. However, if the length of the damage zone is large enough, the calculated value of K_I can noticeably change over the damage zone length scale. It was shown that taking into account the gradient was necessary to achieve correlation in crack jump length between specimens of different geometry [5]. Indeed, for smaller craze zones, when $K_{I,mean}$ was less than 1.0 MPa(m)$^{1/2}$, the data fit the expected squared dependence, the dashed line in Fig. 12. However, for larger craze zones, when $K_{I,mean}$ was greater than 1.0 MPa(m)$^{1/2}$, the zone size deviated from the squared dependence. Consequently, the data were best fit by $da \propto K^{1.5}_{I,mean}$.

3.6. Crack growth rate

The data revealed that damage zone length (da) was proportional to $K^{1.5}_{I,mean}$, and damage zone duration (dt) was proportional to $K^{2.0}_{I,mean}$ and $K^{-4.5}_{I,max}$. Therefore a power law relation in the form:

$$\frac{da}{dt} = BK^{4.5}_{I,max}K^{-0.5}_{I,mean} \qquad (2)$$

should describe the data. Fig. 15 shows da/dt for all the data, including additional results of constant $R = 0.1$ tests, plotted against $K^{4.5}_{I,max}\ K^{-0.5}_{I,mean}$. The data followed a straight line fit with a slope B of 0.5. Equation 2 described all the data for creep, constant $K_{I,mean}$, constant $K_{I,max}$, and constant $R = 0.1$ tests.

As a check of Equation 2, $\log da/dt$ was plotted vs. $\log K_{I,max}$ in Fig. 16a for the data under constant $K_{I,mean} = 0.85$ and 0.72 MPa(m)$^{1/2}$. A linear relation was obtained over the entire range of $K_{I,max}$ with a slope of 4.5. Increasing $K_{I,max}$ decreased dt without affecting da, and therefore da/dt was strongly dependent on $K_{I,max}$. In Fig. 16b, $\log da/dt$ is plotted vs. $\log K_{I,mean}$ for tests under constant $K_{I,max} = 1.30$ and 1.08 MPa(m)$^{1/2}$. Again a linear relation was observed over the entire range of $K_{I,mean}$ and the slope was about

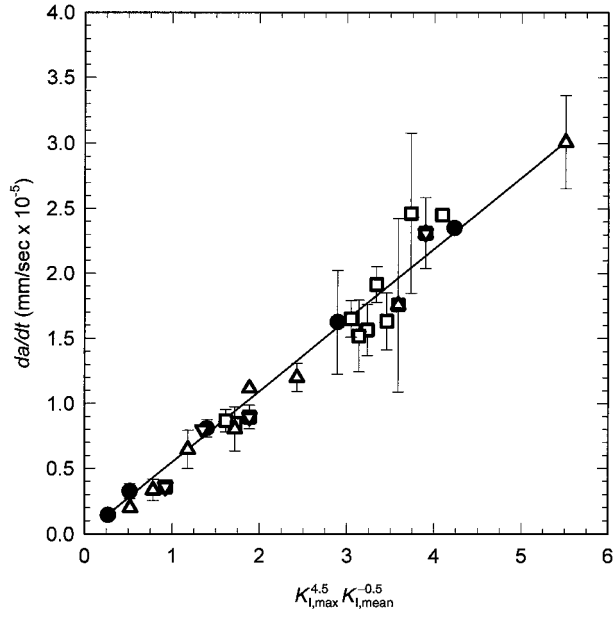

Figure 15 Fit of crack growth rate (da/dt) to the relation $K^{4.5}_{I,max}\ K^{-0.5}_{I,mean}$ for creep (●), constant $K_{I,max}$ (□), constant $K_{I,mean}$ (△), and constant $R = 0.1$ (▽) tests.

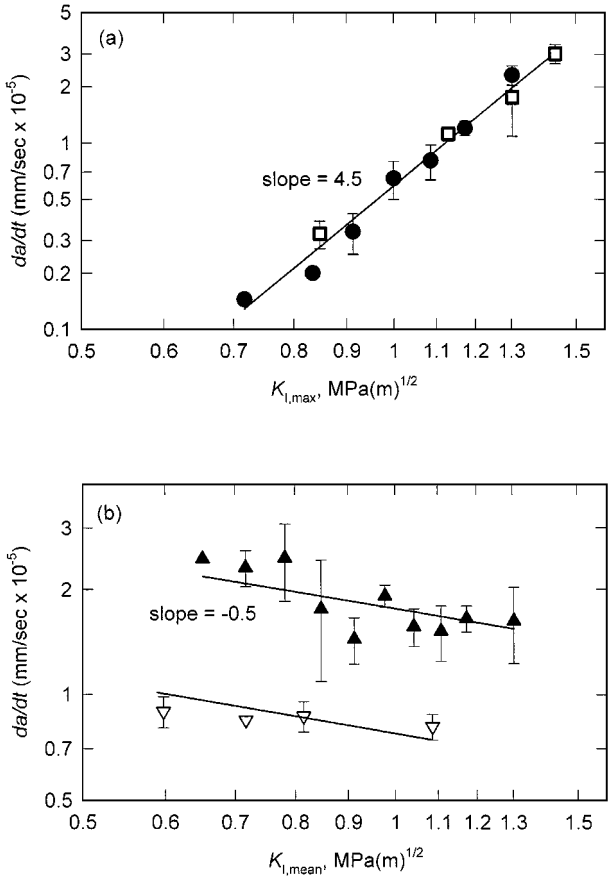

Figure 16 Fits of crack growth rate to (a) $K^{4.5}_{I,max}$ for tests under constant $K_{I,mean}$ of 0.72 MPa(m)$^{1/2}$ (●) and 0.85 MPa(m)$^{1/2}$ (□), and (b) to $K^{-0.5}_{I,mean}$ for tests under constant $K_{I,max}$ of 1.30 MPa(m)$^{1/2}$ (▲) and $K_{I,max} = 1.08$ MPa(m)$^{1/2}$ (▽).

-0.5. Increasing $K_{I,mean}$ increased the step jump length (da), but also increased the damage zone lifetime (dt). The net result was that crack growth rate was only weakly dependent on $K_{I,mean}$, as demonstrated by the exponent $n = -0.5$.

For the creep tests ($K_I = K_{I,max} = K_{I,mean}$) Equation 2 reduces to $da/dt = BK_I^4$. Fig. 17 shows a plot of da/dt vs. log K_I for the five creep experiments. The data fit this relation with a slope $n = 4$, which is consistent with prior studies on creep crack propagation in polyethylene [30–32].

Fatigue crack growth of HDPE under constant $R = 0.1$ was previously found to be described by the Paris relation:

$$\frac{da}{dN} = A\Delta K_I^4 \tag{3}$$

where A is a material constant. Comparison of Equations 2 and 3 can be made if it is realized that of the fatigue loading parameters $K_{I,max}$, $K_{I,min}$, $K_{I,mean}$, ΔK_I, and R there are only two independent variables. Both Equations 2 and 3 can be rewritten as a proportionality between da/dt and $K_{I,max}^4$ or da/dt and $K_{I,mean}^4$ with prefactors that are functions only of R. Therefore, in a series of experiments under constant R, crack growth rate can be described by either Equation 2 or Equation 3. Additionally, the prefactors may depend on fatigue frequency, which was not varied in the present series of experiments [21].

However, fatigue crack growth under varying R cannot be described by the Paris relation, Equation 3. This point is illustrated by constructing a Paris plot, Fig. 18, of the crack growth rate for all the experiments. The Paris relation cannot be applied to creep tests because $\Delta K_I = 0$. However, for comparison, the creep data are shown on the figure as arrows on the ordinate. The fatigue data clearly did not fit Equation 3 with the established value of $n = 4$ (solid line). The results of the present study indicated that a wide range of loading

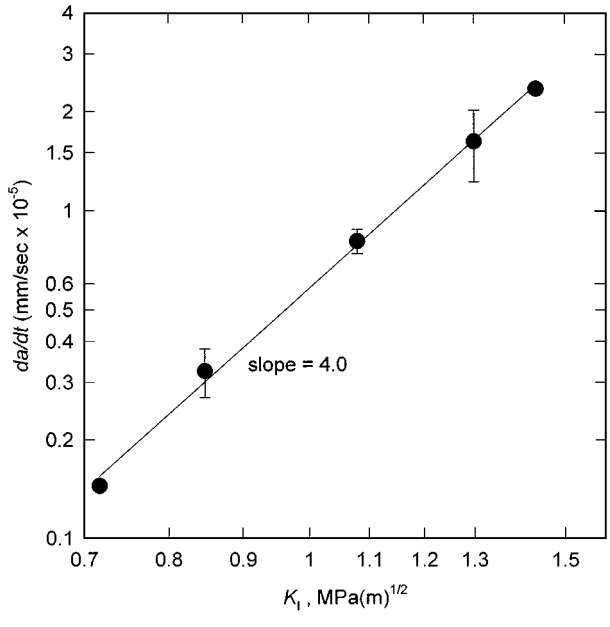

Figure 17 Fit of creep crack growth rate to K_I^4.

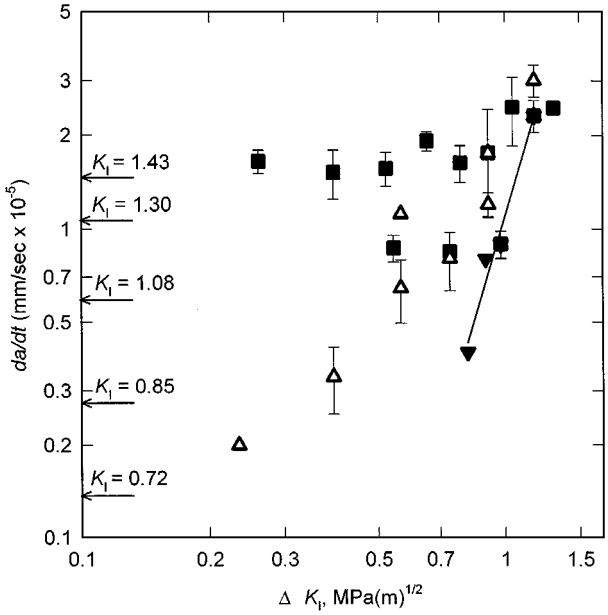

Figure 18 Paris plot of crack growth rate (da/dt) vs. ΔK_I for fatigue tests under constant $K_{I,max}$ (■), constant $K_{I,mean}$ (△), and constant $R = 0.1$ (▽). Arrows indicate creep crack growth rates under different K_I in MPa(m)$^{1/2}$.

conditions is necessary in order to develop a model that fully describes stepwise crack growth in fatigue.

Two other proposed power law relations for fatigue crack growth rate that represent stress intensity by $(K_{I,max}^2 - K_{I,min}^2)^n$ [13] and by $(K_{I,mean}^m \Delta K_I^n)$ [14] may also be expressed as a product of $K_{I,max}^n$ or $K_{I,mean}^n$ and a function of R-ratio. These equations can describe crack growth rate for a constant R if $R < 1$. However, as was the case with the Paris relation, they cannot be extended to describe creep crack growth.

Finally, two limitations of the proposed power law relation, Equation 2, are discussed. First, R must be greater than zero in order to avoid a compressive stress on craze fibrils [20, 21]. Second, the crack propagation mechanism must be stepwise. It is well known that the transition from slow brittle-type crack growth to fast ductile crack growth affects fatigue crack growth kinetics in polyethylene [10, 21, 24]. Consequently, Equation 2 cannot describe ductile fatigue crack growth of HDPE.

4. Conclusions

Stepwise crack propagation in HDPE was observed in tests under both constant maximum stress and constant mean stress loading with R-ratios between 0.1 and 1.0. Crack growth rate in fatigue extrapolated to the case of creep crack growth under both constant maximum and constant mean stress loading. The conservation in stepwise crack growth mechanism and correlation between failure kinetics in fatigue and creep tests suggested that short-term fatigue testing can be used to predict long-term creep failure properties. The damage zone size (da) ahead of the crack tip was determined only by the mean stress. The lifetime of the damage zone (dt) was controlled by the maximum and mean stresses. A relation in the form $da/dt = BK_{I,max}^{4.5} K_{I,mean}^{-0.5}$ described

crack growth rate over the entire range of fatigue and creep loading conditions.

Acknowledgement

The authors gratefully acknowledge the Gas Research Institute for their financial support.

References

1. N. BROWN and X. LU, in Proceedings of the 12th Plastic Fuel Gas Pipe Symposium, Boston, MA, 1991, p. 128.
2. A. SHAH, E. V. STEPANOV, G. CAPACCIO, A. HILTNER and E. BAER, *J. Polym. Sci: Part B: Polym. Phys.* **36** (1998) 2355.
3. A. SHAH, E. V. STEPANOV, M. KLEIN, A. HILTNER and E. BAER, *J. Mater. Sci.* **33** (1998) 3313.
4. *Idem.*, in 1997 Symposium on Plastic Piping Systems for Gas Distribution, Orlando, FL, 1997, p. 235.
5. A. SHAH, E. V. STEPANOV, A. HILTNER, E. BAER and M. KLEIN, *Int. J. Fracture* **84** (1997) 159.
6. A. SHAH, E. V. STEPANOV, A. HILTNER, E. BAER and A. MOET, in SPE Conference Proceedings/54th ANTEC'96, Vol. 3, Indianapolis, IN, 1996, p. 3289.
7. R. W. HERTZBERG and J. A. MANSON, "Fatigue of Engineering Plastics" (Academic Press, New York, 1980).
8. J. A. SAUER and M. HARA, "Advances in Polymer Science," Vol. 91/92 (Springer-Verlag, Berlin, 1990) p. 69.
9. J. C. RADON, *Int. J. Fracture* **16** (1980) 533.
10. C. B. BUCKNALL and P. DUMPLETON, *Polym. Eng. Sci.* **25** (1985) 313.
11. Y. ZHOU and N. BROWN, *ibid.* **33** (1993) 1421.
12. M. D. SKIBO, R. W. HERTZBERG, J. A. MANSON and S. L. KIM, *J. Mater. Sci.* **12** (1977) 531.
13. S. ARAD, J. C. RADON and L. E. CULVER, *J. Mech. Eng. Sci.* **13** (1971) 75.
14. B. MUKHERJEE and D. J. BURNS, *Experimental Mechanics* **11** (1971) 433.
15. S. A. SUTTON, *Eng. Fract. Mech.* **6** (1974) 587.
16. Y. M. MAI and J. G. WILLIAMS, *J. Mater. Sci.* **14** (1979) 1933.
17. N. J. MILLS and N. WALKER, *Polymer* **17** (1976) 335.
18. J. A. MANSON and R. W. HERTZBERG, *CRC Crit. Rev. Macromol. Sci.* **1** (1973) 433.
19. K. YAMADA and M. SUZUKI, *Kobunshi Kagaku* **30** (1973) 206.
20. Y. Q. ZHOU and N. BROWN, *J. Mater. Sci.* **24** (1989) 1458.
21. *Idem., J. Polym. Sci: Part B: Polym. Phys.* **30** (1992) 477.
22. F. VAN DER GRINTEN and P. W. M. WICHERS SCHREUR, *Plast. Rub. Composites Proc. Appl.* **25** (1996) 294.
23. Y. ZHOU, X. LU and N. BROWN, *Polym. Eng. Sci.* **31** (1991) 711.
24. H. NISHIMURA, A. NAKASHIBA, M. NAKAKURA and K. SASAI, *ibid.* **33** (1993) 895.
25. E. SHOWAIB and A. MOET, *J. Mater. Sci.* **28** (1993) 3617.
26. X. LU, R. QIAN and N. BROWN, *ibid.* **26** (1991) 881.
27. L. KÖNCZÖL, M. G. SCHINKER and W. DÖLL, *ibid.* **19** (1984) 1605.
28. D. S. DUGDALE, *J. Mech. Phys. Solids* **8** (1960) 100.
29. J. R. RICE, in "Fracture," Vol. 2, edited by H. Liebowitz (Academic Press, New York, 1968) p. 191.
30. N. BROWN and X. LU, *Polymer* **36** (1995) 543.
31. *Idem., Int. J. Fracture* **69** (1995) 371.
32. P. A. O'CONNELL, M. J. BONNER, R. A. DUCKETT and I. M. WARD, *Polymer* **36** (1995) 2355.

Received 29 December 1998
and accepted 27 January 1999